Electronic Supplementary Information (ESI)

Distinct Magnetic Dynamic Behavior for Two Polymorphs of the Same Dy(III) Complex

Dong-Ping Li,[a] Xiao-Peng Zhang, Tian-Wei Wang, Bin-Bin Ma, Cheng-Hui Li,* Yi-Zhi Li, Xiao-Zeng You*

State Key Laboratory of Coordination Chemistry, School of Chemistry and Chemical Engineering, Nanjing National Laboratory of Microstructures, Nanjing University, Nanjing 210093, P. R. China.

[a] *Present address: Department of Chemistry, Nanchang University, 999 Xuefu Avenue, Nanchang 330031, P. R. China*

Experimental details

Synthesis

The rear-earth β-diketone dihydrate $Dy(NTA)_3 \cdot 2H_2O$ was synthesized by a published methods (see main text). Other reagents were purchased from commercial suppliers and used as received.

Preparation of 1a: An ethanol solution (6 ml) of $Dy(NTA)_3 \cdot 2H_2O$ (NTA = naphthyltrifluoroacetonate, 0.05 mmol) was added to a solution of L (L = (1R,2R)-1,2-diphenylethane-1,2-diamine, 0.05 mmol) in 6 ml acetone under stir. The resultant solution was filtered and placed undisturbed for two weeks. Sheet crystals of **1a** suitable for X-ray diffraction analysis were isolated (yield ca. 45% based on $Dy(NO_3)_3$). Anal Calc for **1** ($C_{56}H_{40}DyF_9N_2O_6$): C, 57.47; H, 3.44; N, 2.39; Found: C, 57.50; H, 3.52; N, 2.37%. IR (KBr, cm^{-1}): 3406(m), 1611(s), 1533(m), 1461 (w), 1303(s), 1190(s), 1138(s), 977(m), 794(m), 572(w), 472(w).

Preparation of 1b: An ethanol solution (3 ml) of $Dy(NTA)_3 \cdot 2H_2O$ (0.05 mmol) was added to a solution of L (0.05 mmol) in 9 ml dichloromethane under stir. The resultant solution was filtered and placed undisturbed for one month. Block crystals of **2** suitable for X-ray diffraction analysis were isolated [yield *ca*. 30% based on

$Dy(NO_3)_3$]. Anal Calc for **2** ($C_{56}H_{40}DyF_9N_2O_6$): C, 57.47; H, 3.44; N, 2.39; Found: C, 57.48; H, 3.49; N, 2.38%. IR (KBr, cm^{-1}): 3418(m), 1612(s), 1532(m), 1462 (w), 1302(s), 1199(s), 1139(s), 977(m), 792(m), 685(m), 573(w), 472(w).

X-ray crystallography. X-ray structure determination for 1a and 1b were carried out on a Bruker SMART APEX CCD diffractometer at room temperature. The data integration and empirical absorption corrections were performed by SAINT program. The structures were solved produced by direct methods and refined anisotropically on F^2 by full-matrix least-squares techniques (SHELXL 97). H atoms attached to N atoms were located in a difference density map and refined isotropically. All other hydrogen atoms were generated geometrically and refined isotropically using the riding mode. CCDC: 783990-783991. Selected bond lengths and bond angles for 1a and 1b are listed in Table S2. Complete crystallographic data are included in the CIF files.

Physical property measurements. Elemental analyses for C, H and N of the complexes were performed on a perkin-Elmer 240C analyzer. Infrared spectra were recorded in KBr pellet on a vector22 Bruker spectrophotometer in the range of 4000-400 cm^{-1}. Variable-temperature magnetic susceptibility, zero-field ac magnetic susceptibility measurements and field dependence of magnetization on polycrystalline samples were performed on a Quantum Design MPMS-XL7 SQUID magnetometer. The powder XRD patterns were recorded on a Shimadzu XD-3A X-ray diffractometer. The complex permittivity ε ($\varepsilon=\varepsilon^0 - i\varepsilon^{00}$) was measured on Tonghui TH2828S in the frequency range 10-2000 kHz. Quasi-isothermal ac calorimetric measurements were performed on an AC-calorimeter setup developed by Prof. Dong-Shan Zhou and co-workers (*Macromolecules* **2008**, 41, 7662-7666; *Eur. Phys. J. Special Topics* **2010**,189, 187 – 195). Continuous Shape Measure Analysis was preformed in the website developed by Prof. David Avnir and coworkers. (http://www.csm.huji.ac.il)

Table S1. Selected Bond Lengths (Å) and Angles (°) for **1a** and **1b**

Complex **1a**		Complex **1b**	
Dy(1)-O(1)	2.362(3)	Dy(1)-O(1)	2.353(4)
Dy(1)-O(2)	2.433(3)	Dy(1)-O(2)	2.331(4)
Dy(1)-O(3)	2.288(3)	Dy(1)-O(3)	2.302(4)
Dy(1)-O(4)	2.328(3)	Dy(1)-O(4)	2.261(4)
Dy(1)-O(5)	2.336(3)	Dy(1)-O(5)	2.319(4)
Dy(1)-O(6)	2.288(3)	Dy(1)-O(6)	2.344(3)
Dy(1)-N(1)	2.496(4)	Dy(1)-N(1)	2.554(4)
Dy(1)-N(2)	2.502(4)	Dy(1)-N(2)	2.528(4)
O(1)-Dy(1)-O(2)	69.81(12)	O(1)-Dy(1)-O(2)	66.72(13)
O(1)-Dy(1)-N(1)	69.98(13)	O(1)-Dy(1)-N(1)	70.98(13)
O(1)-Dy(1)-N(2)	93.26(13)	O(1)-Dy(1)-N(2)	72.22(14)
O(2)-Dy(1)-N(1)	122.57(13)	O(2)-Dy(1)-N(1)	132.37(14)
O(2)-Dy(1)-N(2)	74.76(13)	O(2)-Dy(1)-N(2)	81.89(14)
O(3)-Dy(1)-O(1)	81.64(12)	O(3)-Dy(1)-O(1)	92.39(15)
O(3)-Dy(1)-O(2)	139.30(11)	O(3)-Dy(1)-O(2)	132.30(14)
O(3)-Dy(1)-O(4)	72.45(12)	O(3)-Dy(1)-O(4)	71.55(13)
O(3)-Dy(1)-O(5)	80.83(11)	O(3)-Dy(1)-O(5)	80.45(14)
O(3)-Dy(1)-N(1)	69.71(13)	O(3)-Dy(1)-N(1)	68.97(13)
O(3)-Dy(1)-N(2)	136.97(12)	O(3)-Dy(1)-N(2)	133.89(14)
O(4)-Dy(1)-O(1)	87.26(12)	O(4)-Dy(1)-O(1)	107.72(14)
O(4)-Dy(1)-O(2)	77.67(12)	O(4)-Dy(1)-O(2)	74.96(14)
O(4)-Dy(1)-O(5)	118.41(11)	O(4)-Dy(1)-O(5)	108.08(14)
O(4)-Dy(1)-N(1)	138.00(13)	O(4)-Dy(1)-N(1)	140.37(13)
O(4)-Dy(1)-N(2)	150.35(13)	O(4)-Dy(1)-N(2)	154.25(14)
O(5)-Dy(1)-O(1)	142.23(11)	O(5)-Dy(1)-O(1)	138.92(12)
O(5)-Dy(1)-O(2)	138.73(11)	O(5)-Dy(1)-O(2)	143.05(13)
O(5)-Dy(1)-N(1)	72.61(12)	O(5)-Dy(1)-N(1)	68.70(14)
O(5)-Dy(1)-N(2)	77.65(12)	O(5)-Dy(1)-N(2)	83.90(14)
O(6)-Dy(1)-O(1)	145.11(11)	O(6)-Dy(1)-O(1)	134.29(14)
O(6)-Dy(1)-O(2)	75.57(12)	O(6)-Dy(1)-O(2)	73.33(13)
O(6)-Dy(1)-O(3)	124.92(12)	O(6)-Dy(1)-O(3)	131.84(14)
O(6)-Dy(1)-O(4)	81.31(12)	O(6)-Dy(1)-O(4)	81.47(12)
O(6)-Dy(1)-O(5)	70.47(11)	O(6)-Dy(1)-O(5)	70.89(13)
O(6)-Dy(1)-N(1)	136.33(12)	O(6)-Dy(1)-N(1)	129.02(13)
O(6)-Dy(1)-N(2)	81.48(12)	O(6)-Dy(1)-N(2)	81.22(13)
N(1)-Dy(1)-N(2)	68.46(13)	N(1)-Dy(1)-N(2)	64.94(14)

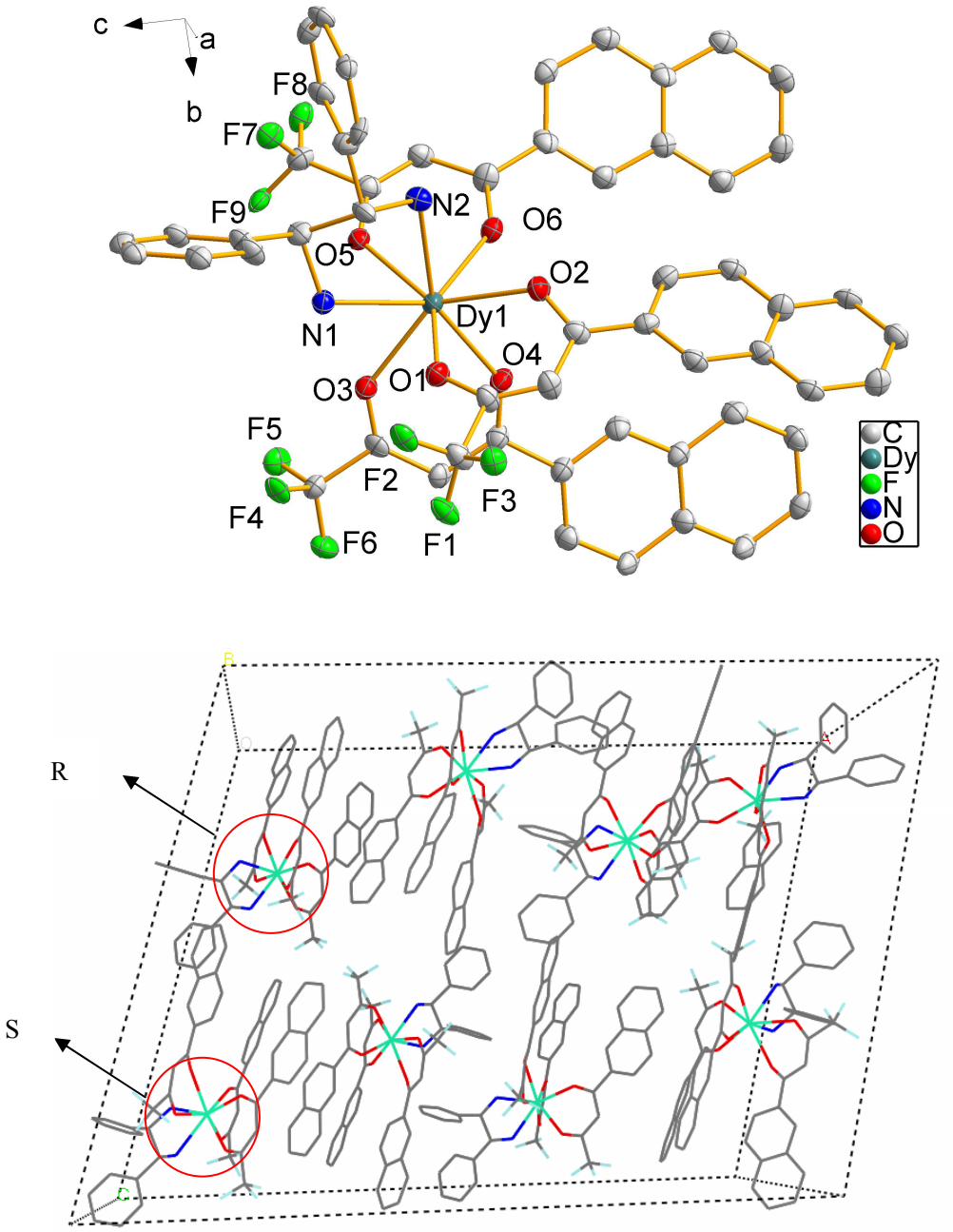

Fig. S1 The molecular structure (up) and packing diagram (down) of complex **1a**. Thermal ellipsoids are drawn at the 30% probability level. H atoms are omitted for clarity.

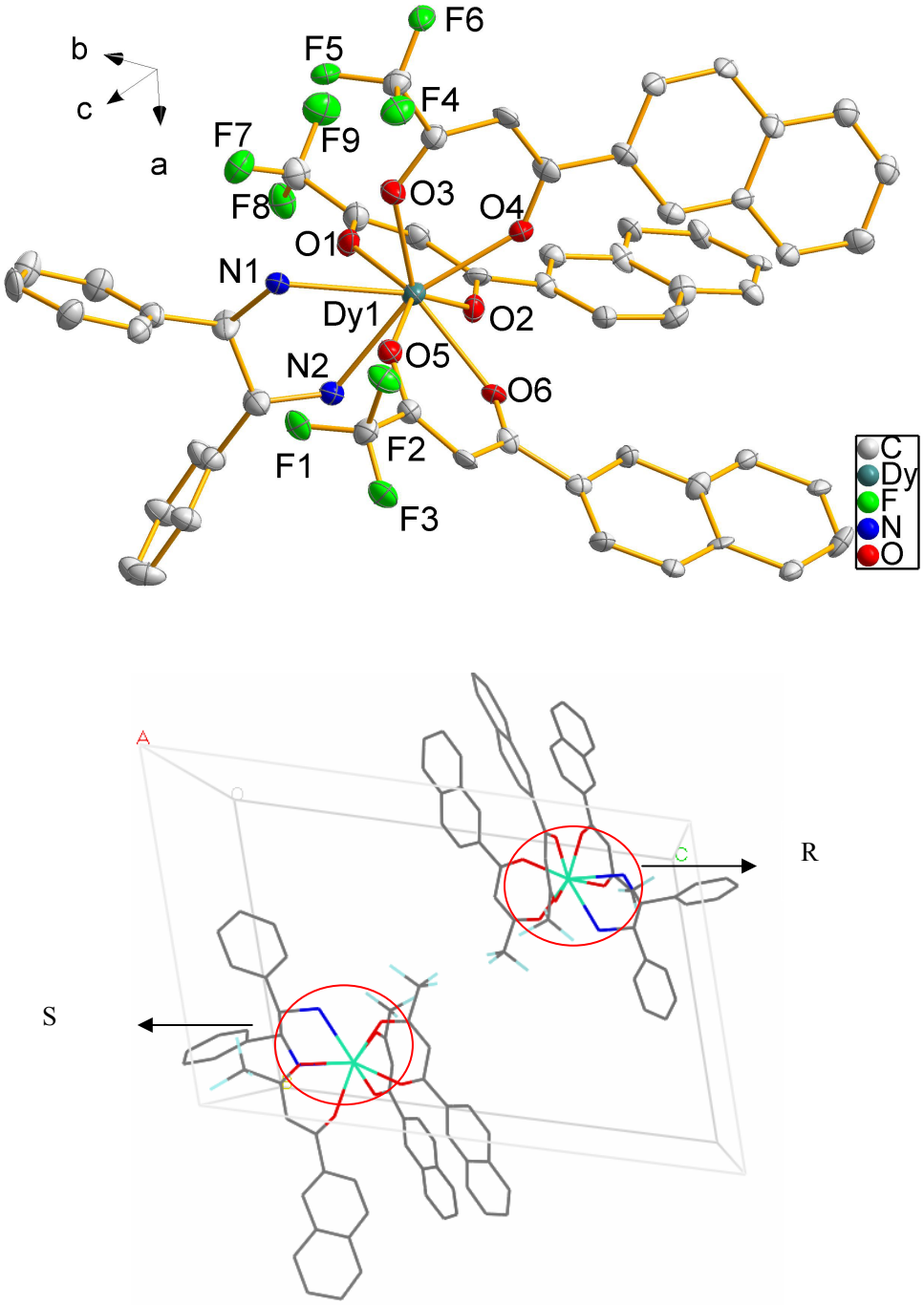

Fig. S2 The molecular structure (up) and packing diagram (down) of complex **1b**. Thermal ellipsoids are drawn at the 30% probability level. H atoms are omitted for clarity.

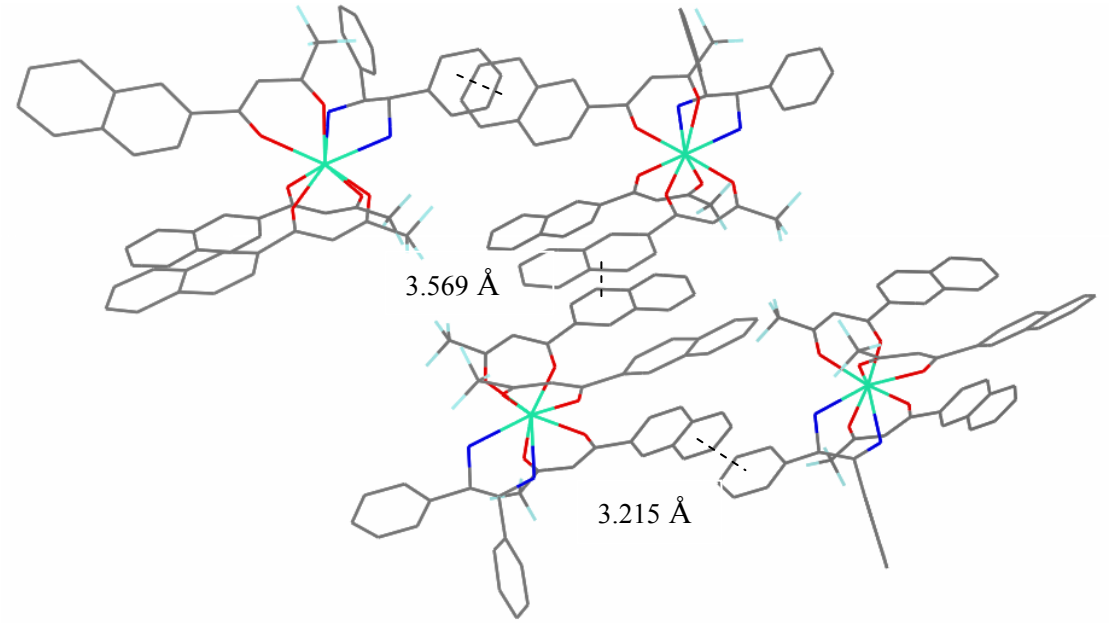

Fig. S3 The π-π stack interactions in complex **1b**. H atoms are omitted for clarity.

Table S2. Results of the Continuous Shape Measure Analysisa geometry[a]

Geometry	S_{SAPR-8}	S_{BTP-8}	S_{DD-8}
1a	1.28	1.25	1.97
1b	3.86	2.47	2.43

[a] S_{SAPR-8} the shape measure relative to the square antiprism, S_{BTP-8} the shape measure relative to the bicapped trigonal prism, and S_{DD-8} is the shape measure relative to the dodecahedron.

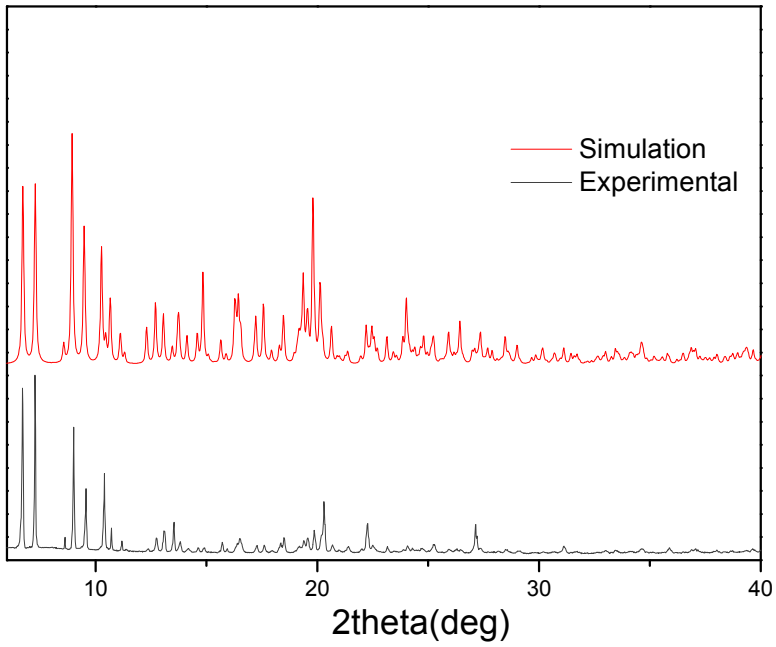

Fig. S4 X-ray powder diffraction patterns for **1a:** red, calculated from single-crystal X-ray data; black, experimental data.

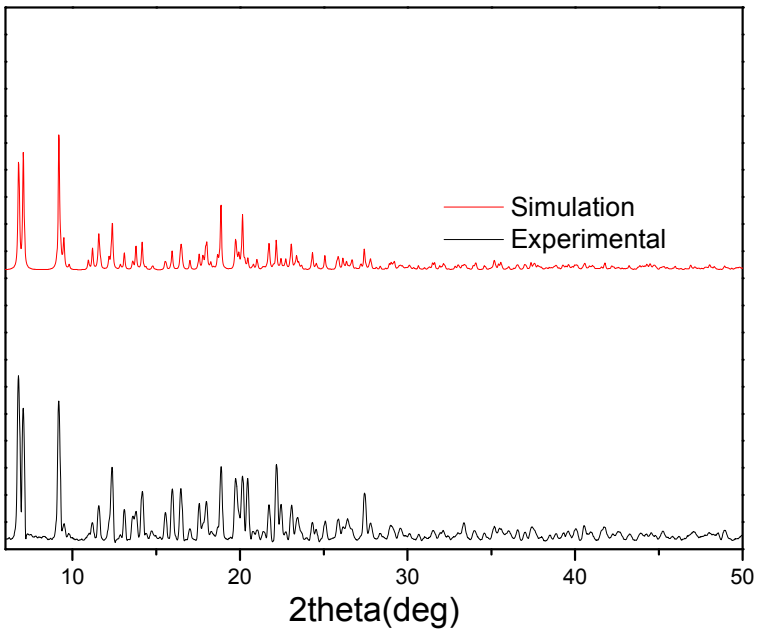

Fig. S5 X-ray powder diffraction patterns for **1b:** red, calculated from single-crystal X-ray data; black, experimental data.

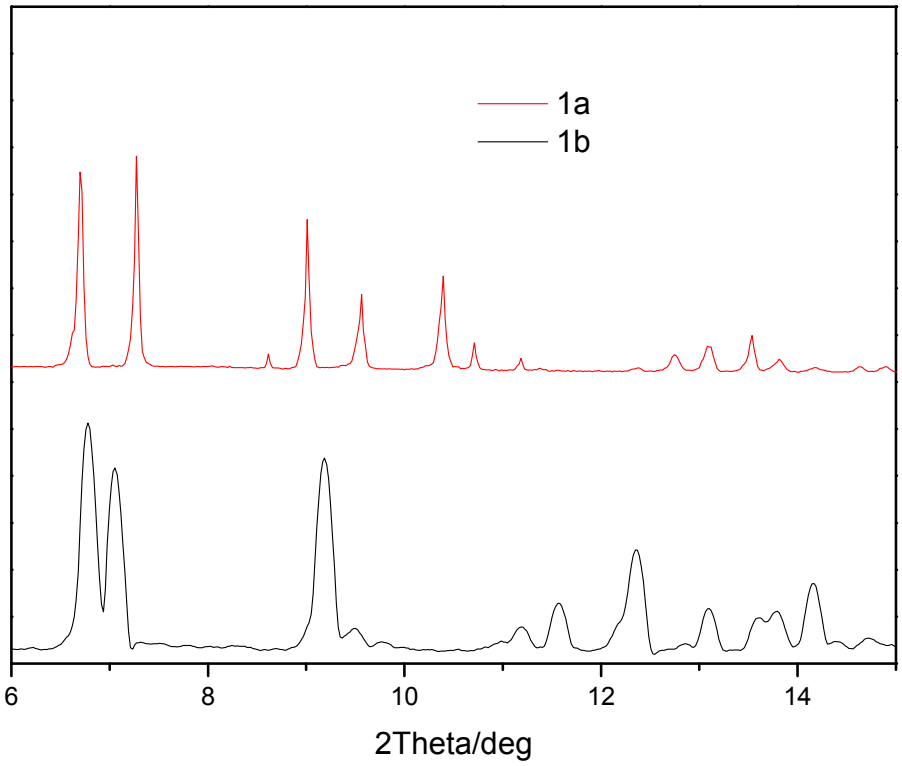

Fig. S6 A comparison of X-ray powder diffraction patterns for **1a** and **1b** at low angle.

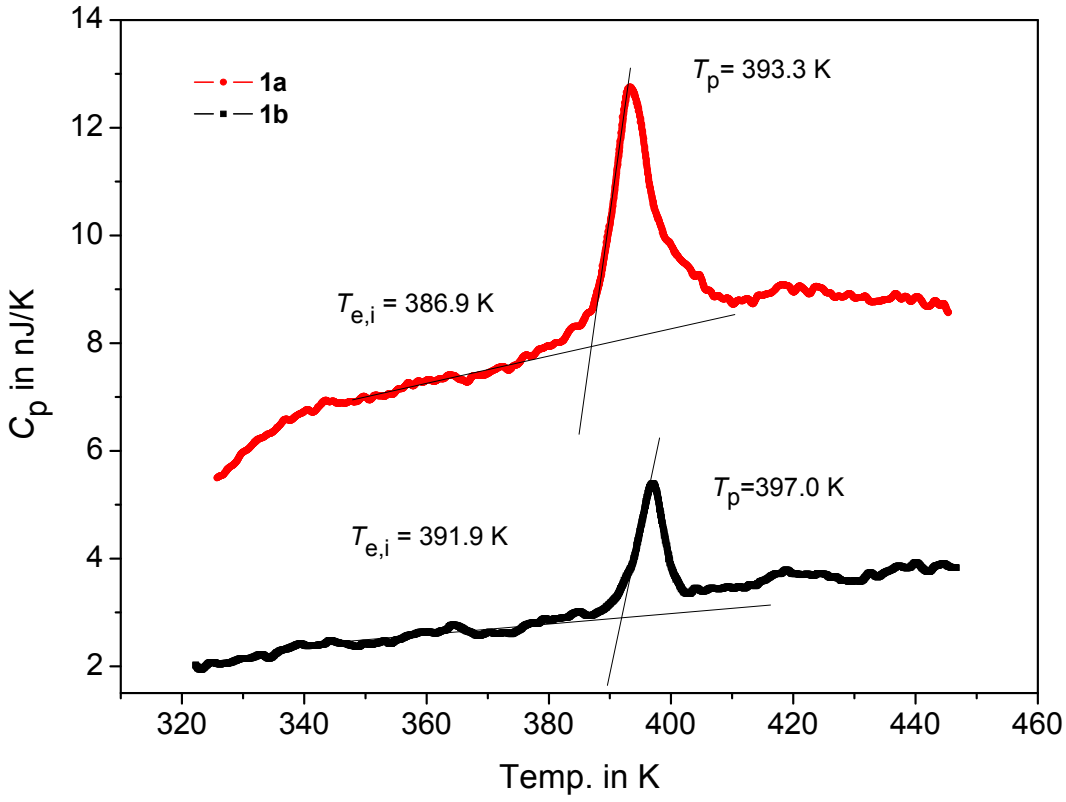

Fig. S7 Amplitude of the complex differential voltage amplitude of **1a** and **1b**.

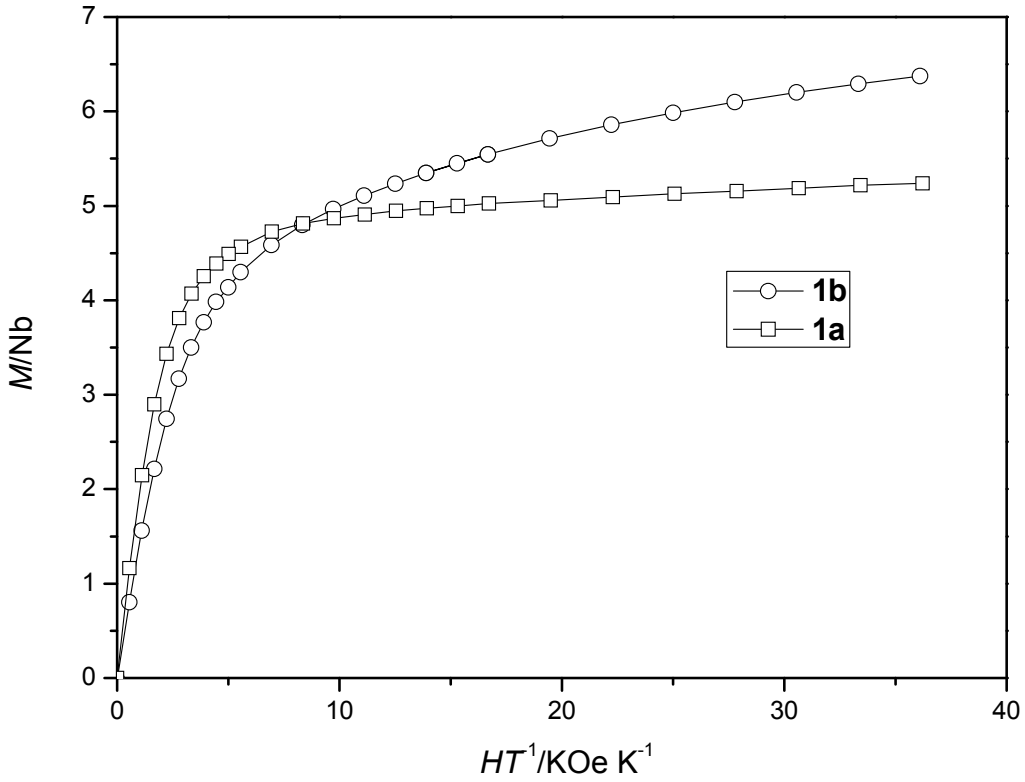

Fig. S8 Magnetization data for **1a** and **1b** at 1.8 K.

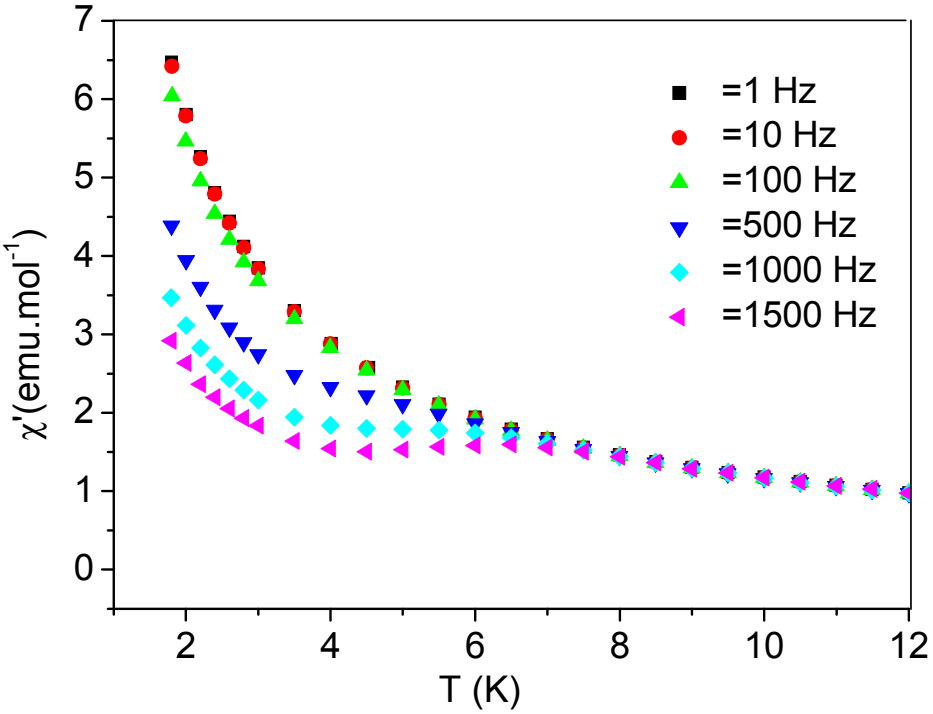

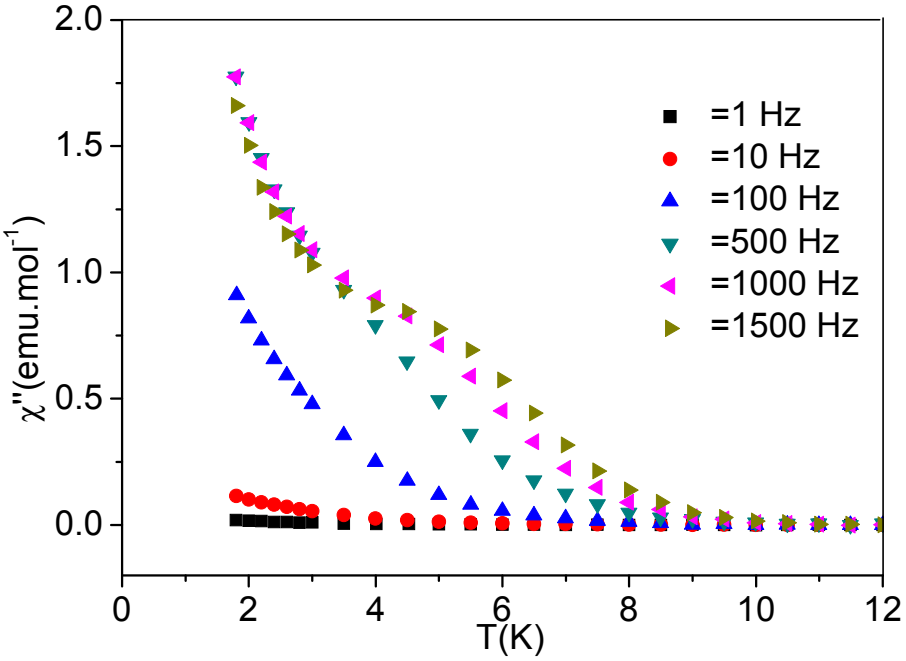

Fig. S9 In-phase (top, χ_m') and out-of-phase (bottom, χ_m'') dynamic magnetic susceptibilities measured in a 3 Oe AC magnetic field with a 2000 Oe dc-field for **1a**.

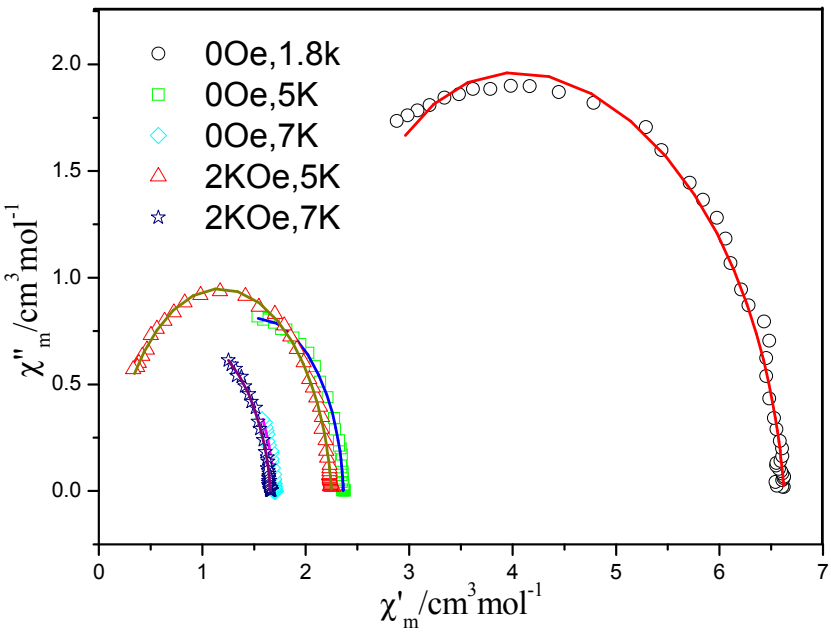

Fig. S10 Cole-Cole plots for ac susceptibility collected under H_{dc} = 0 Oe and 2 kOe for **1a**. The solid lines represent the fitting with a Debye mode. In the plots, α = 0.12, 0.04, 0.06 at 1.8, 5 and 7 K with H_{dc} = 0 Oe; α = 0.08, 0.07 at 5 and 7 K with H_{dc} = 2 kOe.

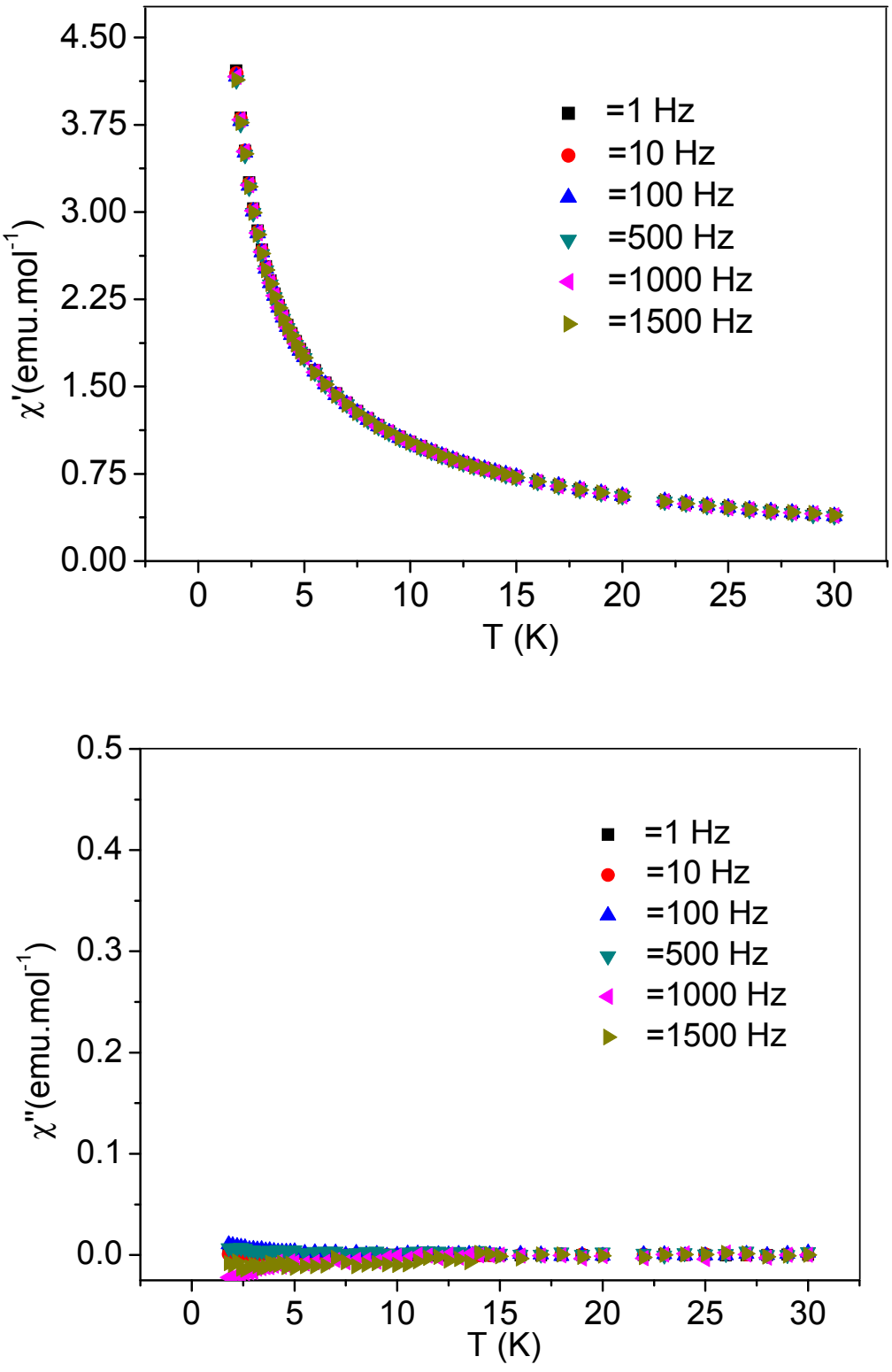

Fig. S11 In-phase (top, χ_m') and out-of-phase (bottom, χ_m'') dynamic magnetic susceptibilities of **1b** measured in a 3 Oe AC magnetic field with a 2000 Oe dc-field.